Hydroxymethylbutenyl diphosphate accumulation reveals MEP pathway regulation for high CO_2-induced suppression of isoprene emission

Abira Sahu [a,b], Mohammad Golam Mostofa [a,b,c], Sarathi M. Weraduwage [a,b,c,d], and Thomas D. Sharkey [a,b,c,1]

[a] Department of Energy Plant Research Laboratory, Michigan State University, East Lansing 48824, Michigan, USA
[b] Plant Resilience Institute, Michigan State University, East Lansing, 48824, Michigan, USA
[c] Department of Biochemistry and Molecular Biology, Michigan State University, East Lansing, 48824, Michigan, USA
[d] Department of Biology and Biochemistry, Bishop's University, Sherbrooke, JIE0L3, Quebec, Canada

[1]**To whom correspondence may be addressed**:
Email: tsharkey@msu.edu

ORCID ID: 0000-0001-9363-6929 (A.S.), 0000-0002-4259-2361 (M.G.M), 0000-0002-0591-4210 (S.M.W.), 0000-0002-4423-3223 (T.D.S.)

Author contributions

T.D.S conceived the experimental plan. A.S. performed the experiments and wrote the first draft of the manuscript. M.G.M and S.M.W assisted in the experimental design, experiments, and production of the manuscript. All authors contributed to manuscript writing and revision, read and approved the submitted version.

The authors declare no competing interest.

Classifications

Biological Sciences; Plant Biology

Keywords: chloroplast; climate change; elevated CO_2; isoprene; MEP pathway

Abstract

Isoprene is emitted by some plants and is the most abundant biogenic hydrocarbon entering the atmosphere. Multiple studies have elucidated protective roles of isoprene against several environmental stresses, including high temperature, excessive ozone, and herbivory attack. However, isoprene emission adversely affects atmospheric chemistry by contributing to ozone production and aerosol formation. Thus, understanding the regulation of isoprene emission in response to varying environmental conditions, for example elevated CO_2, is critical to comprehend how plants will respond to climate change. Isoprene emission decreases with increasing CO_2 concentration; however, the underlying mechanism of this response is currently unknown. We demonstrated that high-CO_2-mediated suppression of isoprene emission is independent of photosynthesis and light intensity, but it is reduced with increasing temperature. Furthermore, we measured methylerythritol 4-phosphate pathway metabolites in poplar leaves harvested at ambient and high CO_2 to identify why isoprene emission is reduced under high CO_2. We found that hydroxymethylbutenyl diphosphate (HMBDP) was increased and dimethylallyl diphosphate (DMADP) decreased at high CO_2. This implies that high CO_2 impeded the conversion of HMBDP to DMADP, possibly through the inhibition of HMBDP reductase activity, resulting in reduced isoprene emission. We further demonstrated that although this phenomenon appears similar to ABA-dependent stomatal regulation, it is unrelated as abscisic acid treatment did not alter the effect of elevated CO_2 on the suppression of isoprene emission. Thus, this study provides a comprehensive understanding of the regulation of the MEP pathway and isoprene emission in the face of increasing CO_2.

Significance statement

Isoprene has significant impacts on air quality and plant health. Because isoprene emission varies with changes in environmental conditions like light, temperature, and CO_2, a mechanistic understanding of the regulation in the face of climate change is essential to predict future isoprene emissions and its effect on the climate. In this study, we characterized CO_2 responsiveness of isoprene at varying light and temperature. We also showed that an increase in upstream precursors but reduction in the immediate precursor of isoprene causes isoprene to decline, indicating an inhibition of a specific enzyme activity at high CO_2. We further demonstrated that high CO_2-mediated suppression of isoprene is independent of the stomatal signaling pathway.

Introduction

Isoprene (C_5H_8, 2-methyl 1,3-butadiene) is a highly reactive, volatile hydrocarbon emitted by various plant species (1, 2). Isoprene accounts for more than half of the total amount of non-methane biogenic volatile organic compounds emitted to the biosphere (3). In the presence of high level of atmospheric nitrogen oxides, an isoprene molecule can contribute to the production of multiple ozone molecules (4). In addition, isoprene is associated with the formation of aerosols, causing appearance of blue haze in the atmosphere (5). According to one estimate, isoprene accounts for nearly 55% of total secondary aerosol production in the eastern United States (6). Therefore, isoprene has significant impacts on tropospheric chemistry by contributing to ozone and secondary aerosol formation and increasing the lifetime of methane (7). Hence, it is crucial to comprehend the physiological mechanisms regulating isoprene emission from plants so that we can predict the effect of isoprene on future atmospheric conditions and how plants will respond to climate changes, such as increasing temperatures and CO_2 concentrations.

In plants, isoprene synthesis begins with the methylerythritol-4-phosphate (MEP) pathway (8, 9). Carbon required for the synthesis of 1-deoxy-D-xylulose-5-phosphate (DXP), the first product of MEP pathway, comes predominantly from the Calvin-Benson cycle (10).This pathway is also dependent on the photosynthetic electron transport chain for the supply of CTP, ATP, NADPH, and ferredoxin. Isoprene is synthesized from dimethylallyl diphosphate (DMADP) by isoprene synthase.

The rate of isoprene emission can vary depending on various environmental factors, including light, temperature, and CO_2. Isoprene emission is light dependent (11, 12) and the light response is similar to that of photosynthesis except that isoprene emission often continues to increase with the increasing illumination even after photosynthesis reaches saturation (13). Isoprene decreases immediately after lights are turned off, indicating the dependence of this phenomenon on the availability of NADPH, ATP, CTP, and ferredoxin from the photosynthetic electron transport chain. Isoprene emission is also affected by temperature variations (12, 14). High temperature leads to increased rates of isoprene emission from plants in both greenhouse and natural settings (14). Isoprene emission also responds to rapid temperature fluctuations (15). Besides light and temperature, CO_2 is another well-studied environmental factor that substantially impacts isoprene emission from plants. In presence of low level of O_2, isoprene emission decreases prominently with increase in CO_2 level (12, 16). However, growing plants in high CO_2 can affect isoprene emission differently depending on the type of plant species. For example, rate of isoprene emission declines in aspen whereas oaks emit more isoprene when they are grown in high CO_2 environment (17). Since both CO_2 levels and temperature are currently on the rise worldwide (18), many models have been created to predict the effect of these two parameters, alone or in combination, on future isoprene emission. Some of these models suggest an increase in isoprene emission by 25-75% in the 21st century (19-21). Based on an IPCC climate model (800 ppm CO_2 and 33°C), Lantz et al (22) predicted that global isoprene emission could increase by as much as 50% by the year 2100 because the effect of high temperature would exceed the inhibition by elevated CO_2.

Multiple studies have been conducted to identify the mechanism behind the high CO_2-mediated inhibition of isoprene emission (22-24). Since isoprene emission is reduced within a few minutes of high CO_2 treatment, changes in gene expression and protein levels are unlikely to explain this reduction. One of the first hypotheses put forward was that an increase in CO_2 concentration stimulates the activity of phosphoenolpyruvate carboxylase (PEPC), leading to a reduction in cytosolic PEP, limiting the availability of pyruvate for the MEP pathway (23). However, inhibition of isoprene emission was not affected at elevated CO_2 upon feeding hybrid poplar leaves with PEPC inhibitors (25). Moreover, PEPC activity was shown to decrease at high CO_2 using stable isotope labeling (26). An alternative hypothesis is that isoprene emission is dependent on the availability of reductive energy equivalents ATP and NADPH (24). ATP and NADPH levels are reduced during feedback inhibition of photosynthesis by high CO_2 due to triose phosphate utilization (TPU) limitation of photosynthesis (27, 28), which could result in lower DMADP levels, reducing the rate of isoprene emission. This is supported by multiple studies showing that isoprene emission is correlated with the DMADP levels in plant tissues (29-31). However, Lantz et al (22) demonstrated that suppression of isoprene emission at high CO_2 is not correlated with TPU limitation. They also suggested that this phenomenon is independent of photosystem (PS)I, PSII, and ATP synthase energetics. Therefore, the underlying mechanism that causes the decrease of isoprene emission at high CO_2 is not clearly understood.

We investigated the effect of light and temperature on the suppression of isoprene emission at elevated CO_2 using gas exchange methods. We found that the CO_2-mediated inhibition of isoprene emission is less at high temperature. Then we used targeted metabolomics of leaves sampled at 41 Pa or 78 Pa CO_2. We found one specific step in the MEP pathway that is inhibited by high CO_2. Stomatal conductance declines at high CO_2 especially in the presence of abscisic acid (ABA), so we tested the effect of ABA on isoprene emission, but ABA did not affect isoprene emission or the response of isoprene emission to CO_2.

Results

Isoprene emission decreases with increasing CO_2 level and is independent of photosynthesis

Photosynthesis and isoprene emission from the leaves were allowed to stabilize at 41 Pa CO_2, 1000 μmol m^{-2} s^{-1} light, and 30°C and then the partial pressure of CO_2 was increased to 78 Pa. Isoprene emission started to decline within 1 min of switching to 78 Pa CO_2 and kept decreasing over time until it stabilized after 20 min of exposure to high CO_2 (Fig. 1A). The average decrease in isoprene emission after switching from 41 to 78 Pa CO_2 was 42 ± 12% (Fig. 1B). Isoprene increased upon returning to 41 Pa CO_2 and stabilized near to the initial value before high CO_2 treatment. Assimilation rates increased by 49 ± 18% (Fig. S1A), whereas stomatal conductance did not show any significant change under these conditions (Fig. S1B). As CO_2 partial pressure was switched from 41 Pa to 78 Pa, photosynthesis increased as quickly as could be detected (within <1 min), whereas isoprene emission declined slowly over a course of 15 min (Fig. 1A). The initial phase of the isoprene decline followed first-order kinetics with a half-life of 6.1 ± 2 min.

Effect of varying light intensity on suppression of isoprene emission at high CO_2

Measurements of CO_2-mediated inhibition of isoprene emission at different light levels were conducted in the same leaf after equilibrating the leaf at 41 Pa CO_2. The decline of isoprene emission at high CO_2 was significant at each light level (Fig. 2A) and the relative decrease in isoprene emission at high CO_2 was similar at different light intensities (Fig. 2B). The absolute change in isoprene emission between 41 and 78 Pa CO_2 increased with increasing light levels and showed significant difference between 100 μmol m^{-2} s^{-1} and 1000 μmol m^{-2} s^{-1} light intensities (Fig. 2C). Assimilation rates increased significantly at 78 Pa CO_2 at each light level; however, the increase was significantly lower at 100 μmol m^{-2} s^{-1} compared with 1000 μmol m^{-2} s^{-1} light intensity (Fig. S2A). The fraction of carbon lost as isoprene was also significantly lower at 78 Pa CO_2 compared with 41 Pa CO_2 at each light level (Fig. S2B).

Effect of temperature on high CO_2-mediated suppression of isoprene emission

Measurements of change in isoprene emission between 41 and 78 Pa CO_2 were conducted at 25°C, 30°C, and 35°C. The high CO_2-mediated decline in isoprene emission was significant at 25°C and 30°C, but not at 35°C (Fig. 2D). Isoprene emission decreased by 61 ± 20% at 25°C and 42 ± 11% at 30°C when CO_2 partial pressure was increased from 41 Pa to 78 Pa (Fig. 2E). However, the decrease of isoprene emission at 35°C under 78 Pa CO_2 was less (18 ± 12%) and it was significantly lower than that observed at 25°C and 30°C (Fig. 2E). The absolute change in isoprene emission was not significantly different at different temperatures (Fig. 2F). Although assimilation rates increased with increase in CO_2 partial pressure, significant difference was not observed in the relative increase of assimilation rates at different temperatures (Fig. S2C). However, the fraction of carbon lost as isoprene was significantly reduced at 78 Pa CO_2 at each temperature (Fig. S2D). Temperature coefficients (Q_{10}) for isoprene emission and assimilation were calculated at 41 Pa and 78 Pa CO_2 (Table 1). Q_{10} value for isoprene emission was 4.6 at 41 Pa CO_2 and 10.3 at 78 Pa CO_2 compared to Q_{10} value of 1.2 for CO_2 assimilation. Therefore, Q_{10} values for isoprene emission was higher than CO_2 assimilation, more so at high CO_2.

Comparison of MEP pathway metabolite levels at 41 and 78 Pa CO_2

Levels of DXP, MEP, 4-(cytidine-5'-diphospho)-2-C-methyl-D-erythritol (CDP-ME), 2-C-methyl-D-erythritol-2,4-cyclodiphosphate (MEcDP), and 4-hydroxy-3-methylbut-2-enyl diphosphate (HMBDP) were quantified using LC-MS/MS in leaf samples collected at the different time points of the isoprene emission curve (Fig. 3A). The level of HMBDP, normalized to DXP, was significantly higher at high CO_2 (Fig. 3B). HMBDP accumulated at T3, and then it decreased at T5 upon returning to 41 Pa CO_2. Since peaks of DMADP were not clearly detectable by LC-MS/MS, the *in vivo* pool size of DMADP was measured by integrating the isoprene emission after turning off the lights. As isoprene emission declined 3 min after switching to high CO_2, DMADP level also started to decrease at T2 and was significantly decreased at T3 compared to T1, when isoprene emission reached a steady minimum at high CO_2 (Fig. 3C). Upon re-exposure to 41 Pa CO_2, DMADP increased 4-fold relative to T3. There was no significant difference in the quantities of other metabolites between 41 and 78 Pa CO_2 (Fig. 3D).

Relationship between high CO_2-mediated suppression of isoprene emission and stomatal signaling

A detached leaf was first fed with water at 41 Pa CO_2 followed by measuring isoprene emission at 78 Pa CO_2 and then 41 Pa CO_2. After isoprene emission stabilized, we fed the leaves with 5 nM ABA and found that there was no change in isoprene emission at 41 Pa CO_2 after feeding the leaves with ABA (Fig. 4A) although stomatal conductance was declined by 11% of its initial value after 15-17 min of ABA feeding (Fig. 4C). Then, the CO_2 partial pressure was increased to 78 Pa. Isoprene emission transiently declined, and photosynthesis increased at 78 Pa CO_2 (Fig. 4B). However, stomatal closure due to ABA eventually resulted in decrease in C_i (Fig. 4D) with a concomitant increase in isoprene (Fig. 4A).

Effect of high CO_2 on H_2O_2 level

Since the [4Fe-4S] cluster of HMBDP reductase (HDR) is susceptible to reactive oxygen species (ROS), we quantified H_2O_2 levels in poplar leaves exposed to 41 or 78 Pa CO_2. Our results indicated a non-significant change in H_2O_2 level between 41 and 78 Pa CO_2 (Fig. S5).

Discussion

The decline in isoprene emission at elevated CO_2 is independent of assimilation rates and varying light intensities; however, it is reduced at high temperature. Isoprene emission decreases at high CO_2 because the DMADP level decreases although the HMBDP level increases. Additionally, high CO_2-mediated inhibition of isoprene emission is independent of the ABA-mediated stomatal signaling pathway. Therefore, our results suggest that high CO_2 signal inhibits the activity of the HDR such that the conversion of HMBDP to DMADP is impeded, resulting in lower isoprene emission at high CO_2 (Fig. 3E).

While CO_2 responsiveness of isoprene emission varies among the species, we observed a 42% decrease in isoprene emission from poplar leaves at elevated CO_2 (Fig. 1B), which corresponded to previous findings (31-33). Our data also indicate that CO_2-mediated suppression of isoprene emission is independent of stomatal conductance (Fig. S1B), consistent with the findings of Jones and Rasmussen (34). Although our experiments show the effect of high CO_2 on isoprene emission for a short time period, multiple studies demonstrated that growing plants at high CO_2 can lead to similar effect on isoprene emission in some species, including *Populus* *deltoides*, *Populus tremuloides*, and *Phragmites* (17, 32, 35). On the contrary, some previous studies (30, 36) showed that there was no change in canopy-level isoprene emission at high CO_2 when the differences in leaf area and biomass were taken into account.

Typically, isoprene biosynthesis relies on photosynthesis for its carbon supply (10, 37). Furthermore, it was observed that ribulose 1,5-bisphosphate (RuBP) and ATP levels decreased, whereas 3-phosphoglyceric acid (PGA) and triose phosphate levels were increased with rising CO_2 concentrations (38). However, the decline of isoprene emission at elevated CO_2 is unrelated to assimilation rates as shown by our data (Fig. 1A). Previously Lantz et al (22) also showed that the decline of isoprene at high CO_2 is independent of TPU limitation, and PSII, PSI, or ATP synthase energetics.

We further explored the impact of environmental conditions like light and temperature on high CO_2-mediated suppression of isoprene emission (Fig. 2). It is evident from earlier studies that isoprene emission increases exponentially with increasing light intensity (11) and the leaves exposed to sunlight emit more isoprene than those in shade (39, 40). Although isoprene emission is light-dependent, it was not clear if illumination level has any impact on the suppression of isoprene emission at elevated CO_2. Our result (Fig. 2A, B) confirmed that the decline of isoprene emission at high CO_2 was independent of the supply of reductive energy equivalents, including ATP and NADPH from the photosynthetic electron transport chain. Furthermore, our results demonstrated that the impact of high CO_2 on isoprene emission was substantially reduced at high temperatures (Fig. 2D, E), which is consistent with previous reports (22, 41, 42). We also showed that decline in isoprene emission at elevated CO_2 was independent of CO_2 assimilation rates since we did not observe any significant difference in relative change of CO_2 assimilation at different temperatures (Fig. S2B). Indeed, temperature response of isoprene is accomplished primarily by regulation of isoprene synthase rather than substrate supply (14, 43). It is interesting that temperature not only regulates absolute rates of isoprene emission (12, 40) but also affects change in isoprene levels at high CO_2 by dampening the suppression of isoprene emission. Arneth et al (44) predicted that CO_2-mediated suppression of isoprene emission is strong enough to offset the increase in emission due to warming climate and increase in plant biomass. Land-use change and vegetation dynamics will also affect future global isoprene emission and some investigators expect that isoprene emission will likely remain the same or decrease in future (45) while others expect increased leaf area index to result in more isoprene emission in a future high

CO_2 world (46). However, Lantz et al (22) estimated an increase in isoprene emission by the year 2100 based on an IPCC climate model (800 ppm CO_2 and 33ºC). Similarly, our results (Fig. 2E) also indicate that isoprene emission will increase under the combined effect of high temperature and elevated CO_2 though without factoring in land use changes and natural vegetation composition. Our study is also based on short-term effects of temperature and CO_2 increase which may have a more severe impact on isoprene emission than compared to a gradual rise in temperature and CO_2, like it is occurring globally. We also observed a remarkable difference in Q_{10} between isoprene emission and CO_2 assimilation (Table 1), which confirms the sensitivity of isoprene to temperature as observed in earlier studies (13, 22). Moreover, Q_{10} of isoprene emission doubled at 78Pa CO_2 compared to 41 Pa CO_2 because of the loss of CO_2 responsiveness of isoprene emission at high temperature. However, regulation of enzyme activities under the combined effect of increased temperature and CO_2 requires further investigation.

Previous studies demonstrated that isoprene emission is correlated with the *in vivo* pool size of DMADP (29, 47, 48). In fact, Niinemets et al (31) showed that DMADP levels decrease at high CO_2 in some species, resulting in reduction of isoprene emission. However, the reason behind the reduced level of DMADP at high CO_2 was not identified. Our data indicate that high CO_2 exposure led to an increase in HMBDP level but a decrease in DMADP pool in poplar leaves, suggesting a possible interruption of HDR activity. It could be due to changes in the intracellular environment that affects the [4Fe-4S] cluster of HDR, leading to reduction in HDR activity. One hypothesis, that H_2O_2 accumulates at high CO_2 was not supported by the data. Therefore, identifying the mechanism of HDR activity regulation at elevated CO_2 remains a pertinent question for future research. A recent study reported the differences in the activities of HDR isoforms in regulation of isoprenoid biosynthesis in other systems (49). Niinemets et al. (31) showed that MEcDP levels were not affected by high CO_2, which is in parallel to our observation. An increase in HMBDP at high CO_2 may also inhibit the activity of DXS (50), which possibly contributed to the insignificant changes in the levels of the metabolites downstream of DXS (Fig. 3D). Thus, our results indicate that HDR activity is a major target of high CO_2-mediated regulation of MEP pathway (Fig. 3E).

There were multiple observations that led us to examine whether the CO_2 sensing mechanism of the stomatal guard cells play a role in regulation of the MEP pathway in the mesophyll cells that leads to the suppression of isoprene emission at high CO_2. First, changes in isoprene emission under varying CO_2 concentrations was similar to the stomatal response (Fig. S4). Next, calcium spikes are associated with stomatal responses; feeding EGTA, a Ca^{2+} chelator, to detached leaves, affects isoprene emission in response to wounding in velvet bean (51). Since stomatal closure at elevated CO_2 requires an ABA-dependent signaling mechanism (52-54) and stomatal closure is accelerated in the presence of ABA and high CO_2 simultaneously (55), we investigated the effect of ABA on the suppression of isoprene emission at high CO_2 to test if similar mechanisms exist in the mesophyll cells that regulate the MEP pathway. We hypothesized that, if the ABA-dependent signaling pathway of stomatal closure at high CO_2 also affected the MEP pathway, then feeding ABA to poplar leaves should exaggerate the CO_2 responsiveness of isoprene emission. Our results (Fig. 4) indicate that the decrease of isoprene emission at high CO_2 is independent of the ABA-dependent stomatal signaling pathway; rather it is entirely regulated by C_i which is consistent with a previous study (56). More information on the different modes of isoprene emission regulation will help developing a large-scale mechanistic model of isoprene emission.

In summary, our study identifies the regulatory point of the MEP pathway under elevated CO_2. This knowledge can be incorporated into the development of predictive models that can more accurately estimate future isoprene emission levels. Thus, we will be able to assess the potential consequences of climate change on isoprene emission from plants and its effect on atmospheric chemistry, plant health, and the ability of plants to adapt to the changing environmental conditions.

Materials and Methods

Plant growth

Poplar 'NM6' hybrid (*Populus nigra X maximowiczii*) plants were grown from stem cuttings provided by the Great Lakes Bioenergy Research Center (GLBRC). The plants were grown in 11-L pots containing Suremix soil (Michigan Grower Products, Galesburg, Michigan, USA) under a greenhouse setting (16 h photoperiod, mean light intensity12 mol m^{-2} d^{-1}, and day/night temperature 33°C/22°C) (Fig. S6). Plants were alternately watered with de-ionized water and half-strength Hoagland's solution every day. Plants were brought from the greenhouse to the lab for conducting experiments. Trees were periodically cut back to provide continuously flushing branches.

Gas exchange studies and isoprene measurement

Gas exchange and isoprene emission measurements were recorded simultaneously using a LI-COR 6800 Portable Photosynthesis System (LI-COR Biosciences, Lincoln, NE) and a Fast Isoprene Sensor (FIS; Hills Scientific, Boulder, Colorado), respectively (57-59). A recently fully expanded mature leaf was used. Exhaust air from the LI-COR 6800 was fed into the FIS for isoprene measurements. The flow rate in the LI-COR 6800 was set at 500 µmol s^{-1} and the FIS flow rate was set such that it drew sample air from the LI-COR 6800 at 600 standard cubic centimeters per min (sccm) (420 µmol s^{-1}). A 3.225 ppm isoprene standard was used for the FIS calibration. First, we determined the background signal by measuring isoprene levels in the air flowing from the empty LI-COR chamber. A leaf was then clamped into a 6 cm^2 chamber and allowed to equilibrate under the following conditions: light intensity of 1000 µmol m^{-2} s^{-1} (50% blue light and 50% red light), temperature of 30°C, CO_2 of 420 µmol mol^{-1} (gases were mixed at different pressures and so are reported as mole fractions here) and water vapor content of 22-26 mmol mol^{-1} depending on laboratory room temperature. Measurements were logged every 5 s for both isoprene and gas exchange parameters.

Harvesting leaves for metabolite analysis

Samples were harvested using an apparatus called Fast Kill freeze clamp that was built in-house and slightly modified from the version used by Li et al (60) (Fig. S3). The LI-COR 6800 head with a 6 cm x 6 cm chamber was mounted on the Fast Kill apparatus. We used cling film wrap to seal the top and bottom to create a closed chamber. Two gooseneck fiber optic illuminators were used to create a uniform field of illumination (1000 µmol m^{-2} s^{-1}). The leaf was clamped in the chamber and allowed to equilibrate under the conditions mentioned above. Leaf temperature was monitored with a thermocouple inserted into the chamber. When both isoprene and assimilation rates stabilized, two copper dies were cooled in liquid nitrogen and put on the apparatus, one above and one below the chamber. The leaf sample was smashed between these two dies. The time between light interruption and when the leaf sample was less than 0°C was measured to be 35 ms. We harvested samples using the gas exchange chamber/freeze clamp at five time points of the isoprene emission curve (Fig. 3A) (i) at 41 Pa CO_2 after isoprene emission stabilized; T1 (ii) 3 min after changing CO_2 to 78 Pa; T2 (iii) at 78 Pa CO_2 after isoprene emission stabilized;

T3 (iv) 3 min after changing CO_2 back to 41 Pa; T4 (v) at 41 Pa CO_2 after isoprene emission stabilized; T5. The samples were stored in -80°C until further analysis.

Extraction of leaf metabolites for LC-MS/MS

Frozen leaf discs were ground into a fine powder in liquid nitrogen using mortar and pestle. Then 500 μL of extraction buffer (3:1:1 acetonitrile: isopropanol: 20 mM ammonium bicarbonate (NH_4HCO_3) adjusted to pH 10 with ammonium hydroxide) was added to the ground plant material. They were then centrifuged at 14,000 g for 10 min. The supernatant was then collected and aliquoted into glass inserts placed in 2 mL glass vials for LC-MS/MS analysis. Samples were analyzed by HPLC immediately after extraction.

Metabolite measurement by LC-MS/MS

Standards of the following compounds DXP, MEP, CDP-ME, MEcDP, and HMBDP were purchased from Echelon Biosciences (Logan, UT, USA). These MEP pathway metabolites were separated using InfinityLab Poroshell 120 HILIC-Z, P column (2.1 x 100 mm, 2.7 micron with column ID) fitted on a Xevo TQ-XS mass spectrometer. Column temperature was set at 25°C. Ammonium bicarbonate (20 mM, adjusted to pH 10.0 with ammonium hydroxide) and acetonitrile were used as mobile phase. A binary gradient was set up as described in Table S1. Negative mode electrospray ionization was used. The following setup was used: capillary 1.00 kV, source temperature of 150°C, and desolvation temperature of 400°C.

DMADP measurement by post illumination isoprene emission

To quantify DMADP from post illumination isoprene emission, we followed the protocol as described by Rasulov et al (61). To differentiate the system response from that of the plant, an isoprene standard of known concentration was injected into the empty leaf chamber using a needle, then the needle was quickly removed to measure the decay kinetics of chamber clearing. Before recording measurements, a poplar leaf was equilibrated under conditions mentioned above. The lights were turned off at the time points T1, T2, T3, T4, and T5 as described above. The difference of area under the curve with and without the plant normalized to the initial isoprene emission was calculated to determine the post illumination isoprene emission from the plant that represents the *in vivo* pool size of DMADP.

ABA feeding

Detached leaves were used for the ABA-feeding experiment. The leaf was cut under water at the base of the petiole using a fresh razor blade. Then it was immediately transferred into a test tube with water or 5 nM ABA for recording measurements, including isoprene emission and CO_2 assimilation following the protocols described above.

Quantification of H_2O_2 level

H_2O_2 levels were quantified using the Amplex Red Assay kit (Amplex Red, DMSO, Horseradish Peroxidase, and 5X phosphate buffer) purchased from Invitrogen (Thermo Fisher Scientific, Waltham, Massachusetts, USA). Plant samples were ground in liquid nitrogen using a tissue homogenizer. Then, the powdered plant material was extracted in 5% trichloroacetic acid for 15 min and centrifuged at 14,000g for 10 min. The supernatant was neutralized with 2.1 M NH_4HCO_3. The extract (5.0 µL) was mixed with 45 µL 1X reaction buffer and 50 µL mix of 100 µM Amplex Red and 0.2 U/mL horseradish peroxidase. The mixture was incubated at room temperature for 30 min in the dark before recording its fluorescence on a microplate reader using 535 nm excitation and 595 nm emission filters. A standard curve was made using a series of H_2O_2 concentrations (0.1 µM, 0.2 µM, 0.4 µM, 0.8 µM, 1 µM, 2.5 µM, 5 µM, and 10 µM) to determine the levels of H_2O_2 in the leaf samples.

Funding

This work was supported by a grant from the National Science Foundation (IOS-2022495) awarded to Thomas D. Sharkey and funds from the MSU Plant Resilience Institute. TDS received partial salary support from Michigan AgBioResearch.

Acknowledgements

We thank Dr. Lijun Chen and Dr. Tony Schilmiller for their assistance with the LC-MS experiment. We also thank Cody Keilen (Growth Chamber Facility, Michigan State University) for his assistance with growth and maintenance of plants, and all members of the Sharkey lab for their support.

Data sharing

All data is available at Dryad DOI 10.5061/dryad.d7wm37q64

References

1. G. Sanadze, A. Kursanov, On certain conditions of the evolution of the diene C_5H_8 from poplar leaves. *Soviet Plant Physiology* **13**, 184-189 (1966).
2. R. A. Rasmussen, Isoprene: identified as a forest-type emission to the atmosphere. *Environmental Science & Technology* **4**, 667-671 (1970).
3. K. Sindelarova *et al.*, Global data set of biogenic VOC emissions calculated by the MEGAN model over the last 30 years. *Atmospheric Chemistry and Physics* **14**, 9317-9341 (2014).
4. T. D. Sharkey, A. E. Wiberley, A. R. Donohue, Isoprene emission from plants: why and how. *Annals of Botany* **101**, 5-18 (2008).
5. F. W. Went, Blue hazes in the atmosphere. *Nature* **187**, 641-643 (1960).
6. Q. Ying, J. Li, S. H. Kota, Significant contributions of isoprene to summertime secondary organic aerosol in eastern United States. *Environmental Science & Technology* **49**, 7834-7842 (2015).
7. X. Lun *et al.*, Reviews of emission of biogenic volatile organic compounds (BVOCs) in Asia. *Journal of Environmental Sciences* **95**, 266-277 (2020).
8. J. Schwender *et al.*, Incorporation of 1-deoxy-D-xylulose into isoprene and phytol by higher plants and algae. *FEBS letters* **414**, 129-134 (1997).
9. J. G. Zeidler, H. K. Lichtenthaler, H. U. May, F. W. Lichtenthaler, Is isoprene emitted by plants synthesized via the novel isopentenyl pyrophosphate pathway? *Zeitschrift für Naturforschung C* **52**, 15-23 (1997).
10. T. D. Sharkey, A. L. Preiser, S. M. Weraduwage, L. Gog, Source of 12C in Calvin–Benson cycle intermediates and isoprene emitted from plant leaves fed with $13CO_2$. *Biochemical Journal* **477**, 3237-3252 (2020).
11. D. T. Tingey, M. Manning, L. C. Grothaus, W. F. Burns, The influence of light and temperature on isoprene emission rates from live oak. *Physiologia Plantarum* **47**, 112-118 (1979).
12. A. T. Lantz, J. Allman, S. M. Weraduwage, T. D. Sharkey, Control of rate and physiological role of isoprene emission from plants. *Plant, Cell & Environment* **42**, 2808 (2019).
13. T. D. Sharkey, F. Loreto, Water stress, temperature, and light effects on the capacity for isoprene emission and photosynthesis of kudzu leaves. *Oecologia* **95**, 328-333 (1993).
14. R. K. Monson *et al.*, Relationships among isoprene emission rate, photosynthesis, and isoprene synthase activity as influenced by temperature. *Plant Physiology* **98**, 1175-1180 (1992).
15. E. L. Singsaas, T. D. Sharkey, The regulation of isoprene emission responses to rapid leaf temperature fluctuations. *Plant, Cell & Environment* **21**, 1181-1188 (1998).
16. R. K. Monson, R. Fall, Isoprene emission from aspen leaves: influence of environment and relation to photosynthesis and photorespiration. *Plant Physiology* **90**, 267-274 (1989).
17. T. D. Sharkey, F. Loreto, C. F. Delwiche, High carbon dioxide and sun/shade effects on isoprene emission from oak and aspen tree leaves. *Plant, Cell & Environment* **14**, 333-338 (1991).
18. S. Adak, N. Mandal, A. Mukhopadhyay, P. P. Maity, S. Sen, "Current State and Prediction of Future Global Climate Change and Variability in Terms of CO_2 Levels and Temperature" in *Enhancing Resilience of Dryland Agriculture Under Changing Climate: Interdisciplinary and Convergence Approaches*. (Springer, 2023), pp. 15-43.
19. M. Sanderson, C. Jones, W. Collins, C. Johnson, R. Derwent, Effect of climate change on isoprene emissions and surface ozone levels. *Geophysical Research Letters* **30** (2003).
20. J. Lathiere, D. Hauglustaine, N. De Noblet-Ducoudré, G. Krinner, G. Folberth, Past and future changes in biogenic volatile organic compound emissions simulated with a global dynamic vegetation model. *Geophysical Research Letters* **32** (2005).
21. C. Wiedinmyer, X. Tie, A. Guenther, R. Neilson, C. Granier, Future changes in biogenic isoprene emissions: how might they affect regional and global atmospheric chemistry? *Earth Interactions* **10**, 1-19 (2006).
22. A. T. Lantz *et al.*, Isoprene suppression by CO_2 is not due to triose phosphate utilization (TPU) limitation. *Frontiers in Forests and Global Change* **2**, 8 (2019).
23. T. N. Rosenstiel, M. J. Potosnak, K. L. Griffin, R. Fall, R. K. Monson, Increased CO_2 uncouples growth from isoprene emission in an agriforest ecosystem. *Nature* **421**, 256-259 (2003).

24. Ü. Niinemets, J. Tenhunen, P. C. Harley, R. Steinbrecher, A model of isoprene emission based on energetic requirements for isoprene synthesis and leaf photosynthetic properties for Liquidambar and Quercus. *Plant, Cell & Environment* **22**, 1319-1335 (1999).
25. B. Rasulov, E. Talts, I. Bichele, Ü. Niinemets, Evidence that isoprene emission is not limited by cytosolic metabolites. Exogenous malate does not invert the reverse sensitivity of isoprene emission to high CO_2. *Plant Physiology* **176**, 1573-1586 (2018).
26. C. Abadie, G. Tcherkez, In vivo phosphoenolpyruvate carboxylase activity is controlled by CO_2 and O_2 mole fractions and represents a major flux at high photorespiration rates. *New Phytologist* **221**, 1843-1852 (2019).
27. T. D. Sharkey, Photosynthesis in intact leaves of C3 plants: physics, physiology and rate limitations. *The Botanical Review* **51**, 53-105 (1985).
28. A. M. McClain, T. D. Sharkey, Triose phosphate utilization and beyond: from photosynthesis to end product synthesis. *Journal of Experimental Botany* **70**, 1755-1766 (2019).
29. B. Rasulov, K. Hüve, M. Välbe, A. Laisk, U. I. Niinemets, Evidence that light, carbon dioxide, and oxygen dependencies of leaf isoprene emission are driven by energy status in hybrid aspen. *Plant Physiology* **151**, 448-460 (2009).
30. M. Possell, C. N. Hewitt, Isoprene emissions from plants are mediated by atmospheric CO_2 concentrations. *Global Change Biology* **17**, 1595-1610 (2011).
31. Ü. Niinemets, B. Rasulov, E. Talts, CO_2-responsiveness of leaf isoprene emission: Why do species differ? *Plant, Cell & Environment* **44**, 3049-3063 (2021).
32. P. Scholefield *et al.*, Impact of rising CO_2 on emissions of volatile organic compounds: isoprene emission from *Phragmites australis* growing at elevated CO_2 in a natural carbon dioxide spring. *Plant, Cell & Environment* **27**, 393-401 (2004).
33. Z. Sun, Ü. Niinemets, K. Hüve, B. Rasulov, S. M. Noe, Elevated atmospheric CO_2 concentration leads to increased whole-plant isoprene emission in hybrid aspen (*Populus tremula*× *Populus tremuloides*). *New Phytologist* **198**, 788-800 (2013).
34. C. A. Jones, R. A. Rasmussen, Production of isoprene by leaf tissue. *Plant Physiology* **55**, 982-987 (1975).
35. M. J. Wilkinson *et al.*, Leaf isoprene emission rate as a function of atmospheric CO_2 concentration. *Global Change Biology* **15**, 1189-1200 (2009).
36. Z. Sun *et al.*, Enhanced isoprene emission capacity and altered light responsiveness in aspen grown under elevated atmospheric CO_2 concentration. *Global Change Biology* **18**, 3423-3440 (2012).
37. C. F. Delwiche, T. D. Sharkey, Rapid appearance of 13C in biogenic isoprene when $13CO_2$ is fed to intact leaves. *Plant, Cell & Environment* **16**, 587-591 (1993).
38. F. Loreto, T. D. Sharkey, On the relationship between isoprene emission and photosynthetic metabolites under different environmental conditions. *Planta* **189**, 420-424 (1993).
39. P. Harley, A. Guenther, P. Zimmerman, Effects of light, temperature and canopy position on net photosynthesis and isoprene emission from sweetgum (*Liquidambar styraciflua*) leaves. *Tree Physiology* **16**, 25-32 (1996).
40. T. D. Sharkey, E. L. Singsaas, P. J. Vanderveer, C. Geron, Field measurements of isoprene emission from trees in response to temperature and light. *Tree Physiology* **16**, 649-654 (1996).
41. R. K. Monson *et al.*, Interactions between temperature and intercellular CO_2 concentration in controlling leaf isoprene emission rates. *Plant, Cell & Environment* **39**, 2404-2413 (2016).
42. T. D. Sharkey, R. K. Monson, The future of isoprene emission from leaves, canopies and landscapes. *Plant, Cell & Environment* **37**, 1727-1740 (2014).
43. Z. Li, E. A. Ratliff, T. D. Sharkey, Effect of temperature on postillumination isoprene emission in oak and poplar. *Plant Physiology* **155**, 1037-1046 (2011).
44. A. Arneth *et al.*, CO_2 inhibition of global terrestrial isoprene emissions: Potential implications for atmospheric chemistry. *Geophysical Research Letters* **34** (2007).
45. S. Hantson, W. Knorr, G. Schurgers, T. A. Pugh, A. Arneth, Global isoprene and monoterpene emissions under changing climate, vegetation, CO_2 and land use. *Atmospheric Environment* **155**, 35-45 (2017).
46. Z. Sun, Ü. Niinemets, K. Hüve, B. Rasulov, S. M. Noe, Elevated atmospheric CO_2 concentration leads to increased whole-plant isoprene emission in hybrid aspen (*Populus tremula* × *Populus tremuloides*). *New Phytologist* **198**, 788-800 (2013).

47. C. Morfopoulos *et al.*, A model of plant isoprene emission based on available reducing power captures responses to atmospheric CO_2. *New Phytologist* **203**, 125-139 (2014).
48. B. Rasulov, E. Talts, Ü. Niinemets, Spectacular oscillations in plant isoprene emission under transient conditions explain the enigmatic CO_2 response. *Plant Physiology* **172**, 2275-2285 (2016).
49. T. Krause *et al.*, HDR, the last enzyme in the MEP pathway, differently regulates isoprenoid biosynthesis in two woody plants. *Plant Physiology* **192**, 767-788 (2023).
50. A. Banerjee *et al.*, Feedback inhibition of deoxy-D-xylulose-5-phosphate synthase regulates the methylerythritol 4-phosphate pathway. *Journal of Biological Chemistry* **288**, 16926-16936 (2013).
51. F. Loreto, T. D. Sharkey, Isoprene emission by plants is affected by transmissible wound signals. *Plant, Cell & Environment* **16**, 563-570 (1993).
52. C. Chater *et al.*, Elevated CO_2-induced responses in stomata require ABA and ABA signaling. *Current Biology* **25**, 2709-2716 (2015).
53. K. E. Hubbard, R. S. Siegel, G. Valerio, B. Brandt, J. I. Schroeder, Abscisic acid and CO_2 signalling via calcium sensitivity priming in guard cells, new CDPK mutant phenotypes and a method for improved resolution of stomatal stimulus–response analyses. *Annals of Botany* **109**, 5-17 (2012).
54. M. Israelsson *et al.*, Guard cell ABA and CO_2 signaling network updates and Ca^{2+} sensor priming hypothesis. *Current Opinion in Plant Biology* **9**, 654-663 (2006).
55. K. Raschke, Simultaneous requirement of carbon dioxide and abscisic acid for stomatal closing in *Xanthium strumarium L. Planta* **125**, 243-259 (1975).
56. G. Guidolotti, C. Calfapietra, F. Loreto, The relationship between isoprene emission, CO2 assimilation and water use efficiency across a range of poplar genotypes. *Physiologia Plantarum* **142**, 297-304 (2011).
57. S. M. Weraduwage, B. Rasulov, A. Sahu, U. Niinemets, T. D. Sharkey, Measurements to assess isoprene plant hydrocarbon emissions and the methylerythritol pathway. *Biochemical Pathways and Environmental Responses in Plants: Part A*, 211 (2022).
58. A. B. Guenther, A. J. Hills, Eddy covariance measurement of isoprene fluxes. *Journal of Geophysical Research: Atmospheres* **103**, 13145-13152 (1998).
59. D. A. Exton *et al.*, Application of a Fast Isoprene Sensor (FIS) for measuring isoprene production from marine samples. *Limnology and Oceanography: Methods* **8**, 185-195 (2010).
60. Z. Li, T. D. Sharkey, Metabolic profiling of the methylerythritol phosphate pathway reveals the source of post-illumination isoprene burst from leaves. *Plant, Cell & Environment* **36**, 429-437 (2013).
61. B. Rasulov, L. Copolovici, A. Laisk, U. I. Niinemets, Postillumination isoprene emission: in vivo measurements of dimethylallyldiphosphate pool size and isoprene synthase kinetics in aspen leaves. *Plant Physiology* **149**, 1609-1618 (2009).

Figure legends

Fig. 1. Effect of 41 Pa and 78 Pa CO_2 on isoprene emission and photosynthesis in poplar leaves. A, Time course of isoprene emission and photosynthesis as CO_2 level is switched between 41 Pa and 78 Pa in a poplar leaf. B, Isoprene emission recorded in poplar leaves (*n*=14) after they reached a stable value at 41 and 78 Pa CO_2. Asterisks indicate significant decline in isoprene emission at 78 Pa CO_2 compared with ambient CO_2 ($P<0.001$; Student's t-test). Whiskers of the box plots represent 95% confidence interval.

Fig. 2. Effect of different light intensities and temperatures on high CO_2-induced suppression of isoprene emission in poplar leaves. A, Isoprene emission in poplar leaves (*n*=3) at five different light intensities at 41 and 78 Pa CO_2. Temperature was held constant at 30°C. B, Relative and C, absolute changes in isoprene emission in poplar leaves (*n*=3) at 41 Pa and 78 Pa CO_2 under different light intensities. D, Isoprene emission in poplar leaves (*n*=6) at three different temperatures at 41 Pa and 78 Pa CO_2. E, Relative and, F, absolute change in isoprene emission in poplar leaves (*n*=6) between ambient and high CO_2 at different temperatures. Light was held constant at 1000 $\mu mol\ m^{-2}\ s^{-1}$. Asterisks indicate significant decline in isoprene emission at 78 Pa CO_2 compared with 41 Pa CO_2 (* $P<0.05$, ** $P<0.01$, *** $P<0.001$; Student's two-tailed t-test) in A and D. Statistically significant differences by ANOVA and Tukey's HSD ($P<0.001$) are indicated by lowercase letters in B, C, E, and F. Whiskers of the box plots represent 95% confidence interval.

Fig. 3. Change in the levels of MEP pathway metabolites at high CO_2. A, Plot showing time points on the isoprene emission curve where leaf samples were harvested. Levels of B, HMBDP relative to DXP, C, DMADP, and D, other MEP pathway metabolites (MEP, CDP-ME, and MEcDP) measured in poplar leaves (*n*=3-4) at 41 Pa and 78 Pa CO_2 levels. Statistically significant differences by ANOVA and Tukey's HSD ($P<0.05$) are indicated by lowercase letters. E, Schematic representation of isoprene biosynthesis via MEP pathway in chloroplasts and proposed regulatory point of isoprene suppression in high CO_2. Whiskers of the box plots represent 95% confidence interval. Bar plots represent mean ± SD for each group. Abbreviations: DXP = 1-deoxy-D-xylulose-5-phosphate, MEP = methylerythritol 4-phosphate, CDP-ME = 4-(cytidine-5'-diphospho)-2-C-methyl-D-erythritol, MEcDP = 2-C-methyl-D-erythritol-2,4-cyclodiphosphate, HMBDP = 4-hydroxy-3-methylbut-2-enyl-diphosphate, IDP = isopentenyl diphosphate, DMADP = dimethylallyl diphosphate, DXS=1-deoxy-D-xylulose-5-phosphate synthase, DXR=1-deoxy-D-xylulose-5-phosphate reductoisomerase, CMS=4-diphosphocytidyl-2-C-methylerythritol synthase, CMK= 4-(cytidine-50-diphospho)-2-C-methyl-D-erythritol kinase, MCS=2-C-methyl-Derythritol-2,4-cyclodiphosphate synthase, HDS=4-hydroxy-3-methylbut-2-enyl-diphosphate synthase, HDR=4-hydroxy-3-methylbut-2-enyl-diphosphate reductase, IspS=isoprene synthase.

Fig. 4. Relationship between high CO_2-mediated changes of isoprene emission and ABA-dependent stomatal signaling pathway. Absolute change in: A, isoprene emission; B, photosynthesis (*A*); C, stomatal conductance (g_{sw}); and D, intercellular CO_2 concentration (C_i) measured in a poplar leaf at 41 Pa CO_2 and 78 Pa CO_2 levels in the presence of water (control) followed by 5 nM ABA treatment.

CO_2 (Pa)	**Q_{10} isoprene**	**Q_{10} photosynthesis**
41	4.6	1.2
78	10.3	1.2

Table 1: Temperature sensitivity of isoprene emission and photosynthesis. Q_{10} was calculated using the equation:

$$Q_{10} = \left(\frac{R2}{R1}\right)^{(10/(T2-T1))}$$

where T2= 35°C, T1=25°C, and R2 and R1 are the rates of isoprene emission or assimilation measured at 35°C and 25°C respectively.

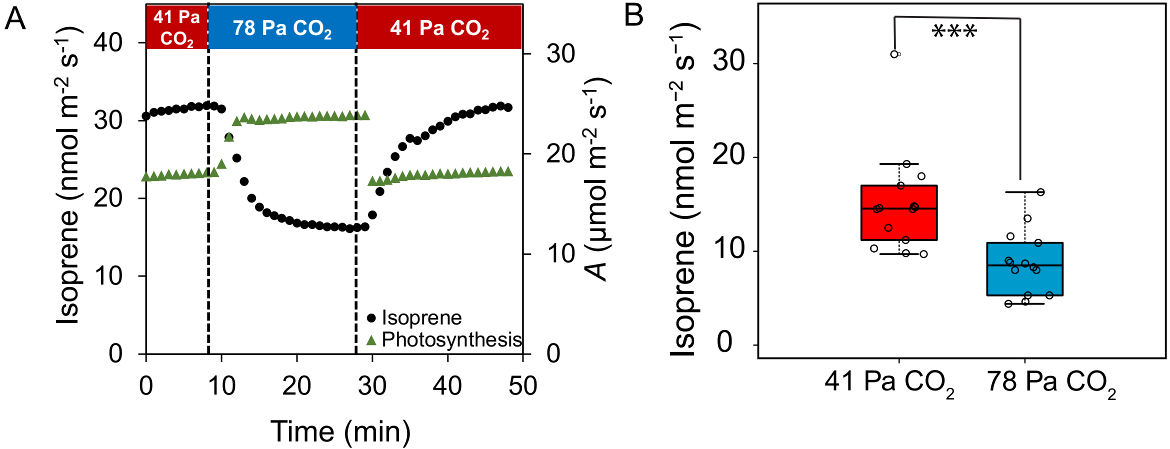
A
41 Pa CO₂
78 Pa CO₂
41 Pa CO₂
Isoprene (nmol m-2 s-1)
40
30
20
10
0
A (µmol m-2 s-1)
30
20
10
0
0
10
20
30
40
50
Time (min)
● Isoprene
▲ Photosynthesis
B
***
Isoprene (nmol m-2 s-1)
30
20
10
0
41 Pa CO2
78 Pa CO2

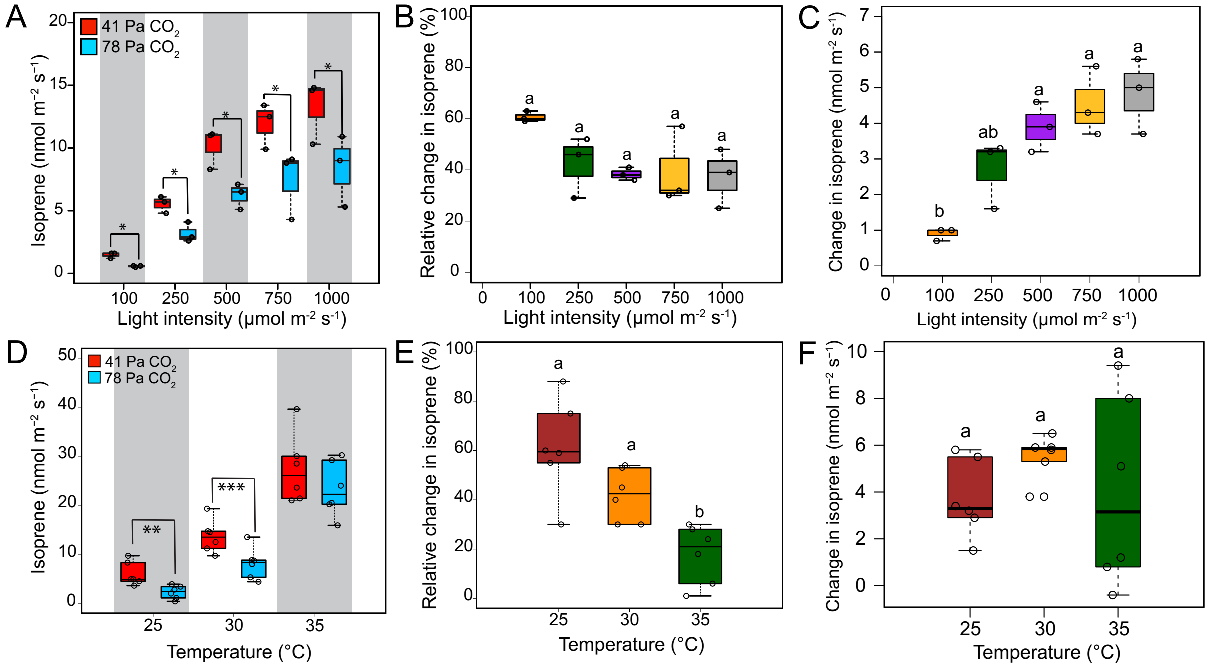
A
41 Pa CO_2
78 Pa CO_2
Isoprene (nmol m^{-2} s^{-1})
0
5
10
15
20
*
100
250
500
750
1000
Light intensity (µmol m^{-2} s^{-1})
B
Relative change in isoprene (%)
0
20
40
60
80
100
a
Light intensity (µmol m^{-2} s^{-1})
C
Change in isoprene (nmol m^{-2} s^{-1})
0
1
2
3
4
5
6
7
b
ab
a
Light intensity (µmol m^{-2} s^{-1})
D
41 Pa CO_2
78 Pa CO_2
Isoprene (nmol m^{-2} s^{-1})
0
10
20
30
40
50
**
***
25
30
35
Temperature (°C)
E
Relative change in isoprene (%)
0
20
40
60
80
100
a
b
Temperature (°C)
F
Change in isoprene (nmol m^{-2} s^{-1})
0
2
4
6
8
10
a
Temperature (°C)

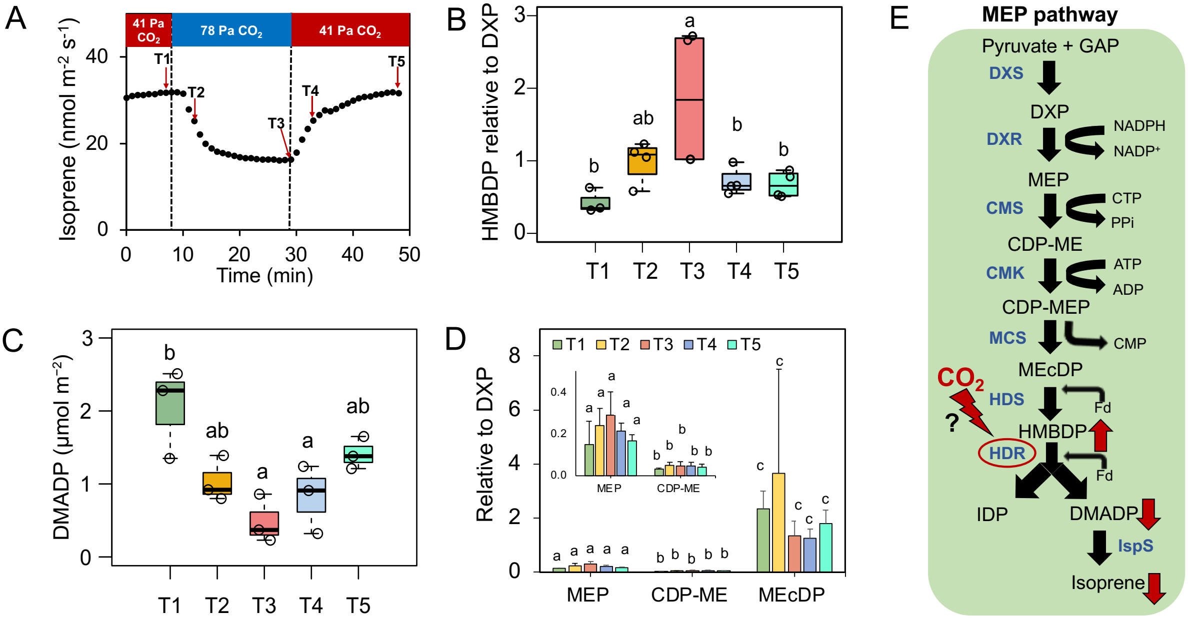
A
41 Pa CO$_2$
78 Pa CO$_2$
41 Pa CO$_2$
Isoprene (nmol m^{-2} s^{-1})
T1
T2
T3
T4
T5
0
20
40
0
10
20
30
40
50
Time (min)
B
HMBDP relative to DXP
0
1
2
3
a
ab
b
b
b
T1
T2
T3
T4
T5
C
DMADP (μmol m^{-2})
0
1
2
3
b
ab
a
a
ab
T1
T2
T3
T4
T5
D
Relative to DXP
🟩T1 🟨T2 🟥T3 🟦T4 🟩T5
0
2
4
6
8
0.0
0.2
0.4
a a a a a
b b b b b
MEP
CDP-ME
a a a a a
b b b b b
c c c c c
MEP
CDP-ME
MEcDP
E
MEP pathway
Pyruvate + GAP
DXS
DXP
DXR
NADPH
NADP$^+$
MEP
CMS
CTP
PPi
CDP-ME
CMK
ATP
ADP
CDP-MEP
MCS
CMP
MEcDP
CO$_2$
HDS
Fd
?
HMBDP
HDR
Fd
IDP
DMADP
IspS
Isoprene

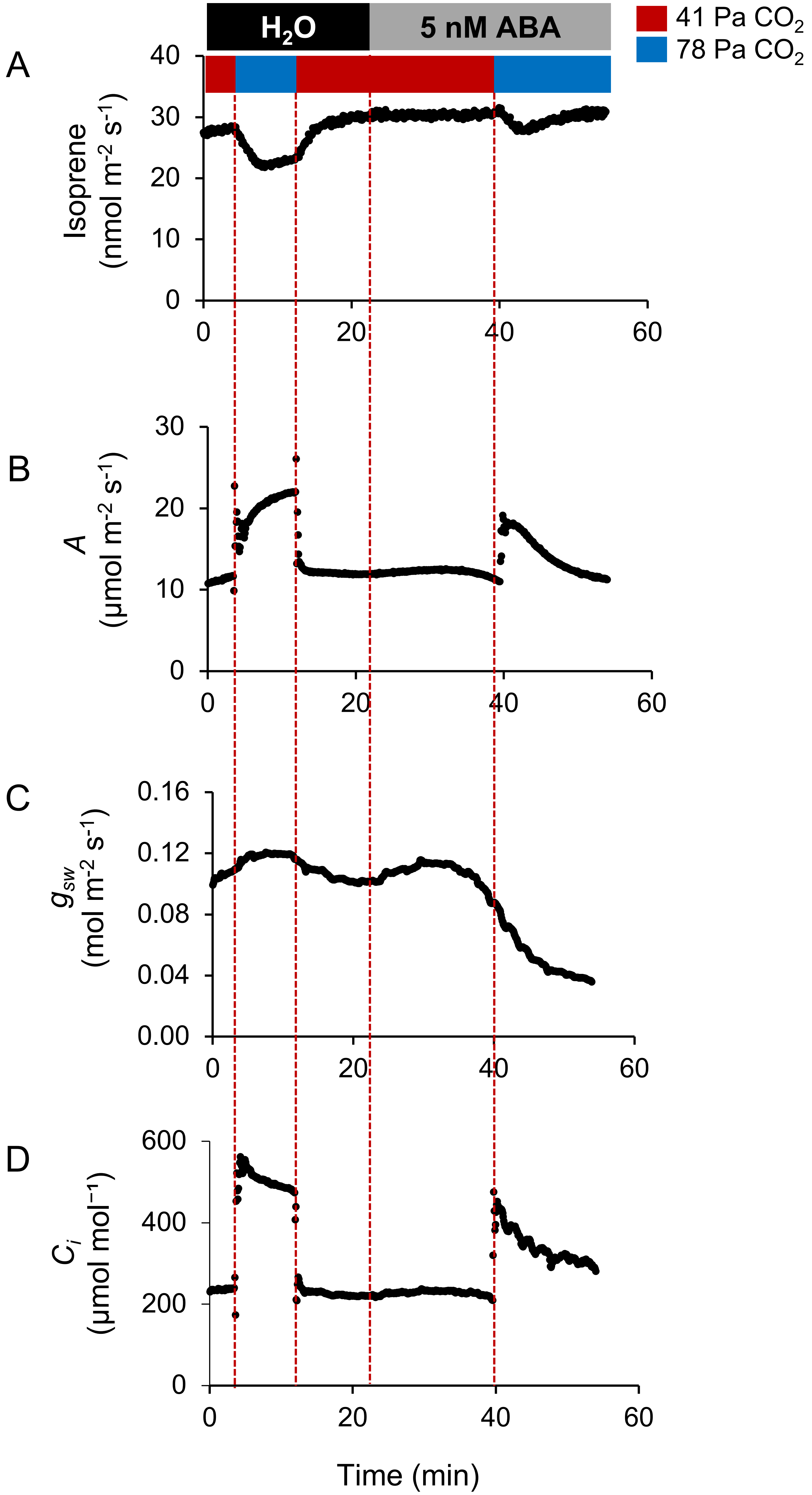H2O
5 nM ABA
41 Pa CO2
78 Pa CO2
A
Isoprene (nmol m-2 s-1)
0
10
20
30
40
0
20
40
60
B
A (µmol m-2 s-1)
0
10
20
30
0
20
40
60
C
gsw (mol m-2 s-1)
0.00
0.04
0.08
0.12
0.16
0
20
40
60
D
Ci (µmol mol-1)
0
200
400
600
0
20
40
60
Time (min)

Hydroxymethylbutenyl diphosphate accumulation reveals MEP pathway regulation for high CO_2-induced suppression of isoprene emission

Abira Sahu [a,b], Mohammad Golam Mostofa [a,b,c], Sarathi M. Weraduwage [a,b,c,d], and Thomas D. Sharkey [a,b,c,1]

[a] Department of Energy Plant Research Laboratory, Michigan State University, East Lansing 48824, Michigan, USA
[b] Plant Resilience Institute, Michigan State University, East Lansing, 48824, Michigan, USA
[c] Department of Biochemistry and Molecular Biology, Michigan State University, East Lansing, 48824, Michigan, USA
[d] Department of Biology and Biochemistry, Bishop's University, Sherbrooke, JIE0L3, Quebec, Canada

Supplementary materials

Fig. S1. Effect of high CO_2 on photosynthesis and stomatal conductance in poplar leaves.
Fig. S2. Effect of different light intensities and temperatures on photosynthesis and carbon cost of isoprene emission at high CO_2.
Fig. S3. Experimental setup for collecting leaf tissue for metabolite analysis.
Fig. S4. Effect of increasing CO_2 on isoprene emission and stomatal conductance (g_{sw}).
Fig. S5. H_2O_2 level in poplar leaves at ambient and high CO_2.
Fig. S6. Growth conditions (light and temperature) maintained in the greenhouse to grow poplar plants.
Table S1. Gradient table for binary solvents consisting of 20 mM NH_4HCO_3 in H_2O, pH~10 used for separation of MEP pathway metabolites.

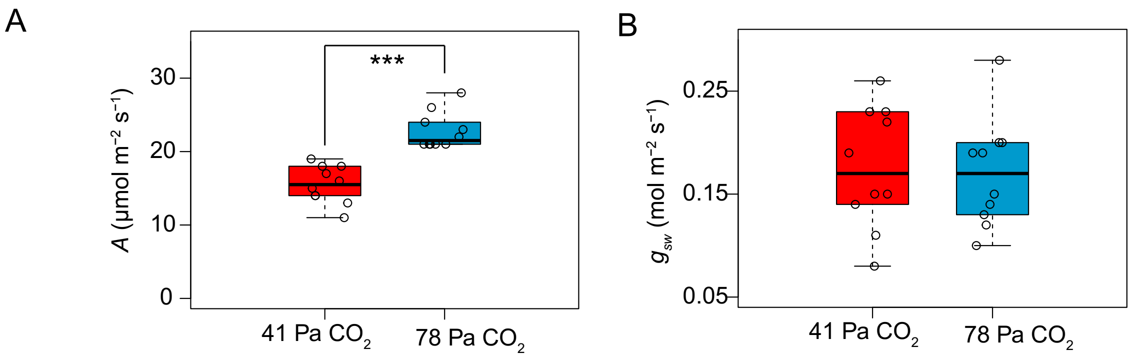

Fig. S1. Effect of high CO_2 on photosynthesis and stomatal conductance in poplar leaves. A, Photosynthesis (*A*); and B, stomatal conductance (g_{sw}) recorded in poplar leaves (*n*=10) after they reached a stable value at 41 Pa and 78 Pa CO_2. Asterisks indicate significant increase in photosynthesis at high CO_2 compared with ambient CO_2 ($P<0.001$; Student's t-test). Whiskers of the box plots represent 95% confidence interval.

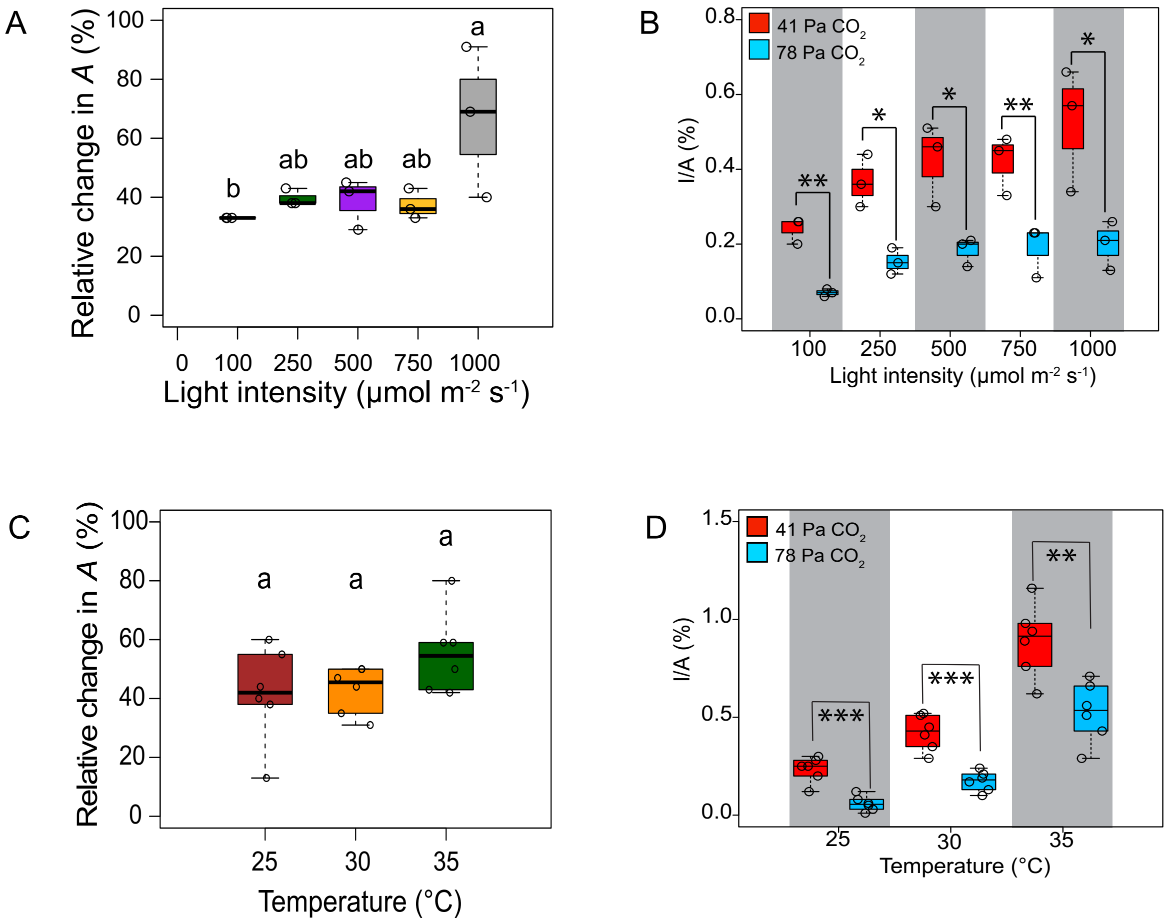

Fig. S2. Effect of different light intensities and temperatures on photosynthesis and carbon cost of isoprene emission at high CO_2. A, Relative change in photosynthesis and B, Carbon lost as isoprene as a fraction of net carbon assimilation between 41 Pa and 78 Pa CO_2 in poplar leaves (*n*=3) at different light intensities; and C, Relative change in photosynthesis and D, Carbon lost as isoprene as a fraction of net carbon assimilation between 41 Pa and 78 Pa CO_2 in poplar leaves (*n*=6) at different temperatures. Statistically significant differences by ANOVA and Tukey's HSD ($P<0.001$) are indicated by lowercase letters in A and C. Asterisks indicate significant decline in isoprene emission at 78 Pa CO_2 compared with 41 Pa CO_2 (* $P<0.05$, ** $P<0.01$, *** $P<0.001$; Student's two-tailed t-test) in B and D. Whiskers of the box plots represent 95% confidence interval.

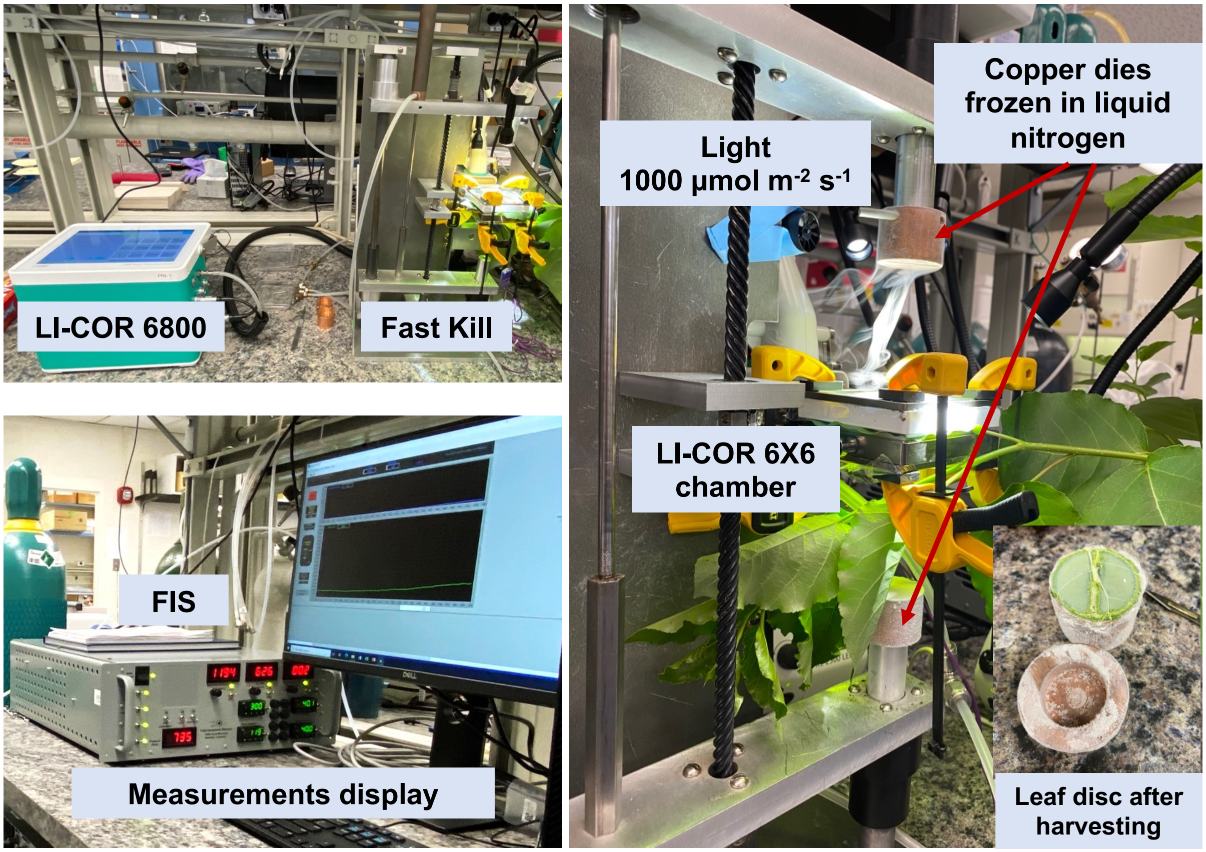

Fig. S3. Experimental setup for collecting leaf tissue for metabolite analysis. A LI-COR head attached to a 6 cm x 6 cm chamber is mounted on the Fast Kill apparatus. A leaf is clamped in the chamber and isoprene emission is monitored using the FIS while simultaneously recording photosynthetic measurements in the LI-COR 6800 console. Copper dies frozen in liquid nitrogen are used to flash freeze leaf discs and collect samples at specific time points.

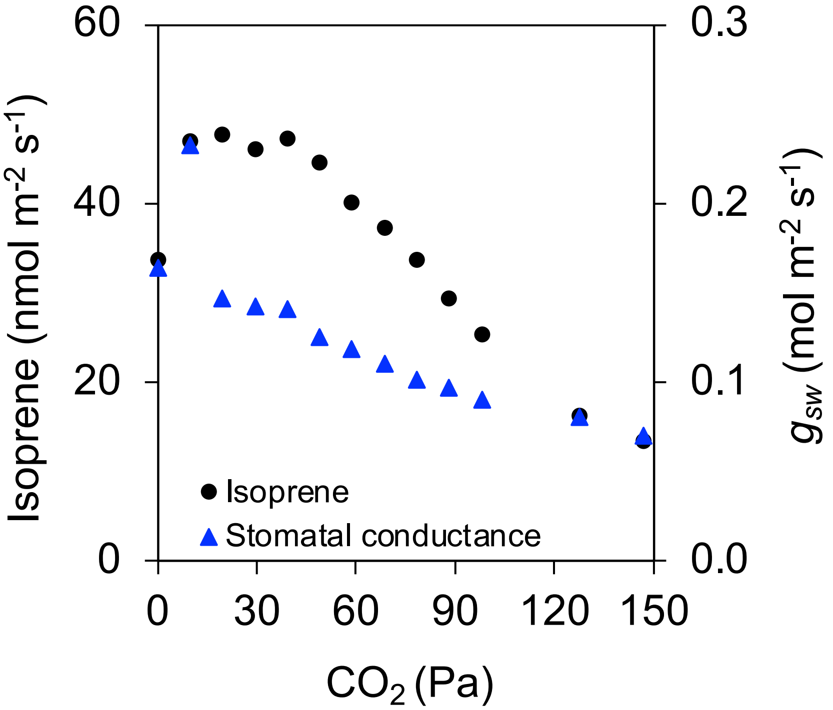

Fig. S4. Effect of increasing CO_2 on isoprene emission and stomatal conductance (g_{sw}).

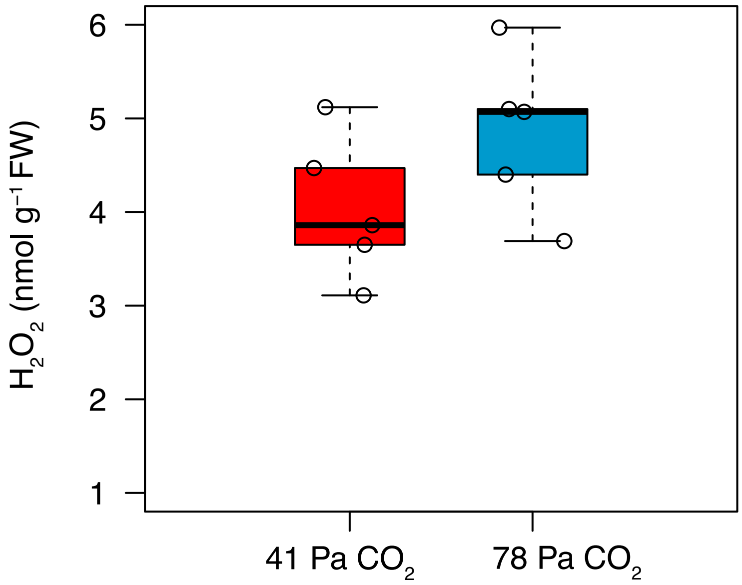

Fig. S5. H_2O_2 level in poplar leaves at ambient and high CO_2. No significant difference in H_2O_2 level was observed. Whiskers of the box plots represent 95% confidence interval.

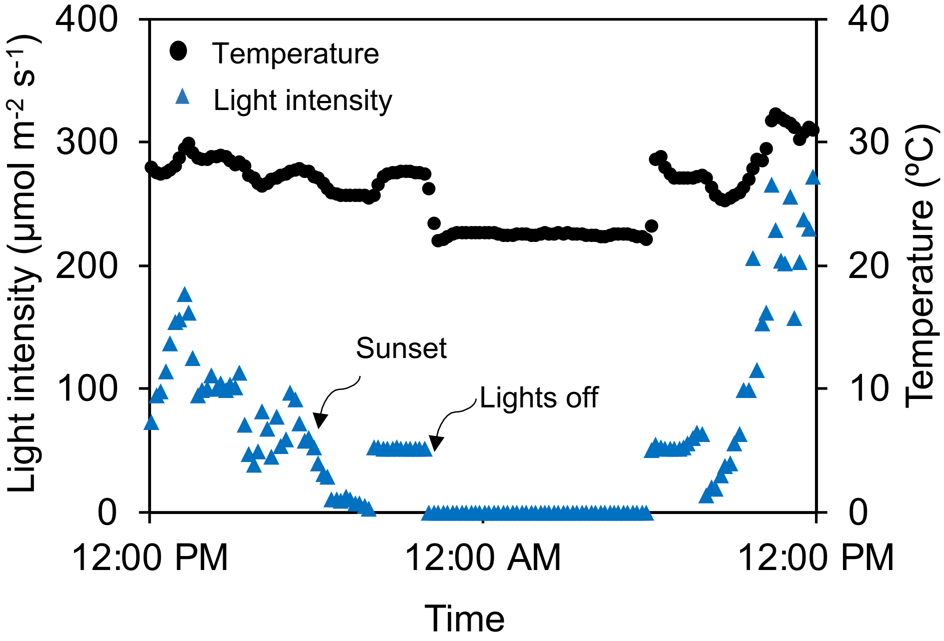

Fig. S6. Growth conditions (light and temperature) maintained in the greenhouse to grow poplar plants.

Time (min)	Flow Rate (mL/min)	%A	%B
0.00	0.2	20	80
2.00	0.2	20	80
6.00	0.2	60	40
8.00	0.2	60	40
8.10	0.2	20	80
10.00	0.2	20	80

A: 20mM NH_4HCO_3 in H_2O, pH~10
B: Acetonitrile

Table S1. Gradient table for binary solvents consisting of 20 mM NH_4HCO_3 in H_2O, pH~10 used for separation of MEP pathway metabolites.